A tryptophan metabolite made by a microbiome eukaryote induces pro-inflammatory T cells

Lukasz Wojciech[1,2], Chin Wen Png[1,2,3], Eileen Y. Koh[2,4], Dorinda Yan Qin Kioh[5], Lei Deng[2,4], Ziteng Wang[5], Liang-zhe Wu[1,2], Maryam Hamidinia[1,2], Desmond W.H. Tung[1,2], Wei Zhang[6], Sven Pettersson[2,6,7,8], Eric Chun Yong Chan[5], Yongliang Zhang[1,2,3], Kevin S.W. Tan*[2,4], and Nicholas R.J. Gascoigne*[1,2,6]

Affiliations

[1]Immunology Translational Research Programme, Yong Loo Lin School of Medicine, National University of Singapore

[2]Department of Microbiology and Immunology, Yong Loo Lin School of Medicine, National University of Singapore, 5 Science Drive 2, Singapore 117545

[3]Immunology Programme, Life Sciences Institute, National University of Singapore, Singapore

[4]Healthy Longevity Translational Research Programme, Yong Loo Lin School of Medicine, National University of Singapore

[5]Department of Pharmacy, Faculty of Science, National University of Singapore, 18 Science Drive 4, Singapore 117543

[6]ASEAN Microbiome Nutrition Centre, National Neuroscience Institute, Singapore

[7]Faculty of Medical Sciences, Sunway University, Subang Jaya, Malaysia

[8]Department of Odontology, Karolinska Institutet, Stockholm, Sweden

*Equal contributions, Co-corresponding authors: micnrjg@nus.edu.sg; mictank@nus.edu.sg

Table of contents

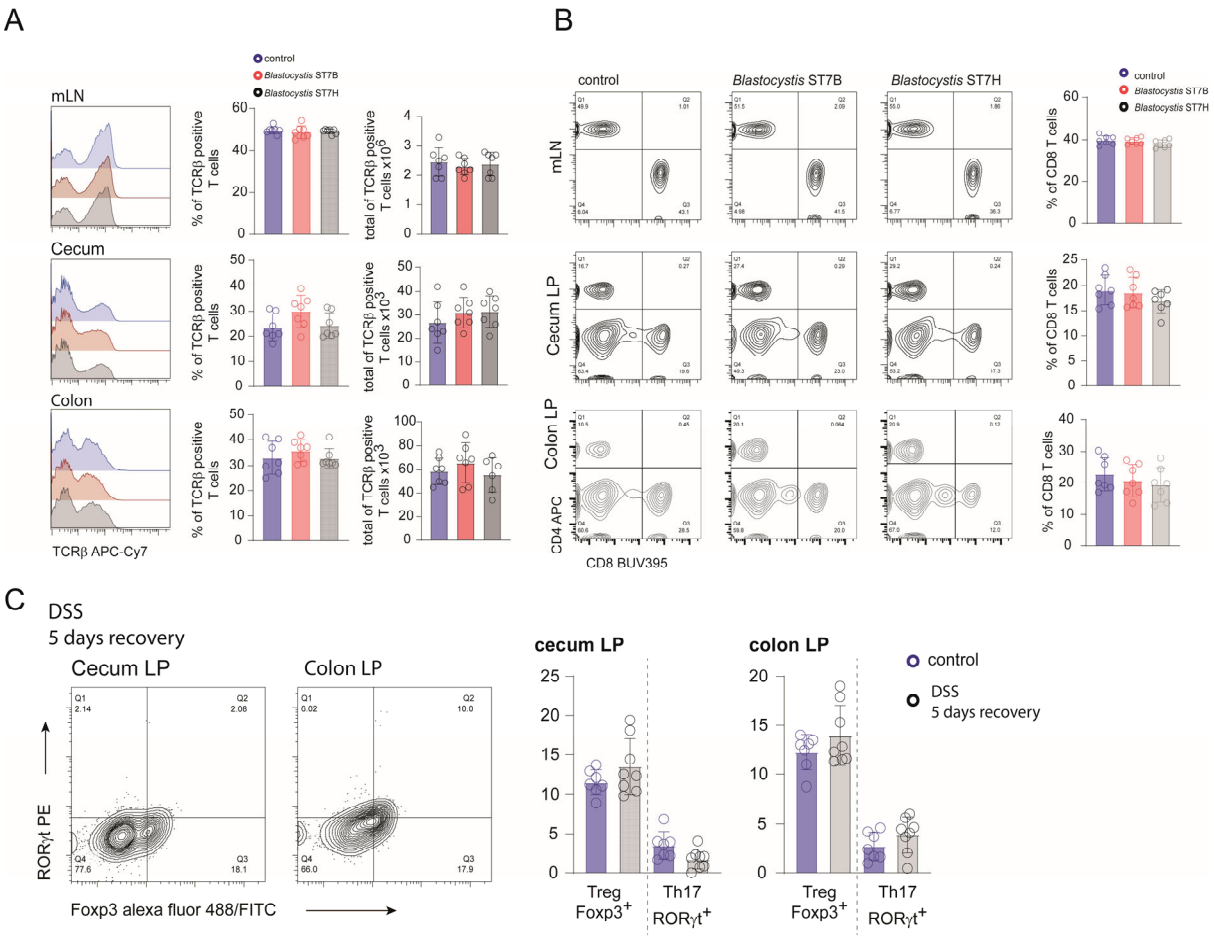

Appendix Fig. S1:

A. Proportion and total number of TCRαβ T cells from the mesenteric LN, cecum and colon lamina propria of control and *Blastocystis* ST7-infected mice. **B**. Distribution of TCRαβ $CD4^+$ and TCRαβ $CD8^+$ T cells in the mesenteric LN, cecum and colon lamina propria of control and *Blastocystis* ST7-infected mice. **C**. TCRαβ $CD4^+$ T cell compartment in cecum and colon lamina propria isolated from animals after DSS colitis induction followed by five days of recovery. This control group comprised eight animals. Statistical analysis was performed using two-tailed t-test with Welch-correction.

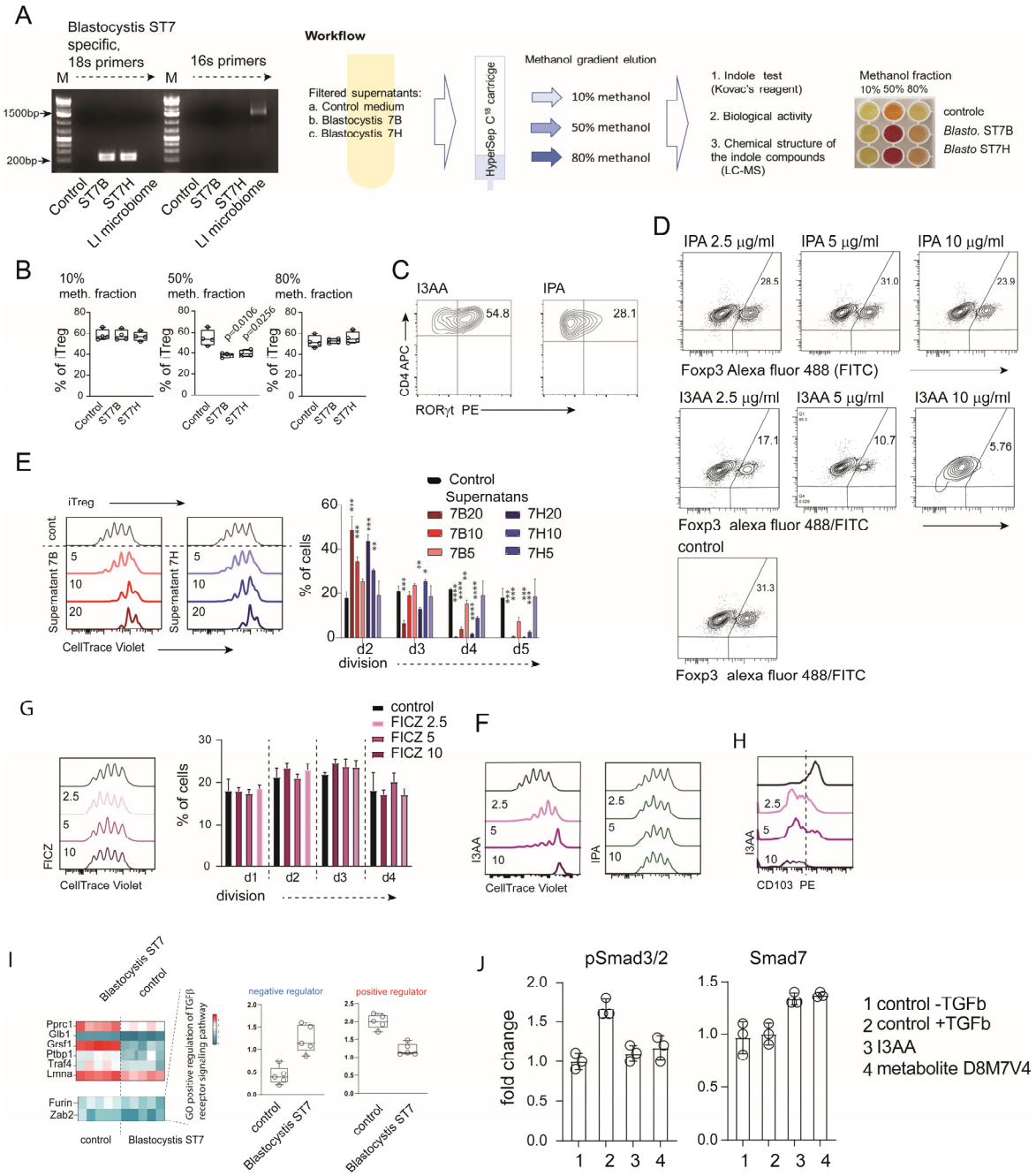
A
Blastocystis ST7 specific, 18s primers
16s primers
1500bp
200bp
Control
ST7B
ST7H
LI microbiome
Workflow
Filtered supernatants:
a. Control medium
b. Blastocystis 7B
c. Blastocystis 7H
HyperSep C18 cartridge
Methanol gradient elution
10% methanol
50% methanol
80% methanol
1. Indole test (Kovac's reagent)
2. Biological activity
3. Chemical structure of the indole compounds (LC-MS)
Methanol fraction
10% 50% 80%
controle
Blasto. ST7B
Blasto ST7H
B
10% meth. fraction
50% meth. fraction
80% meth. fraction
% of iTreg
p=0.0106
p=0.0256
C
I3AA
IPA
54.8
28.1
CD4 APC
RORγt PE
D
IPA 2.5 µg/ml
IPA 5 µg/ml
IPA 10 µg/ml
28.5
31.0
23.9
Foxp3 Alexa fluor 488 (FITC)
I3AA 2.5 µg/ml
I3AA 5 µg/ml
I3AA 10 µg/ml
17.1
10.7
5.76
Foxp3 alexa fluor 488/FITC
control
31.3
Foxp3 alexa fluor 488/FITC
E
iTreg
cont.
Supernatant 7B
Supernatant 7H
CellTrace Violet
Control
Supernatans
7B20
7B10
7B5
7H20
7H10
7H5
% of cells
d2 division
d3
d4
d5
G
control
FICZ 2.5
FICZ 5
FICZ 10
FICZ
CellTrace Violet
% of cells
division
d1
d2
d3
d4
F
I3AA
IPA
CellTrace Violet
H
I3AA
CD103 PE
I
Blastocystis ST7
control
Pprc1
Glb1
Gref1
Ptbp1
Traf4
Lmna
Furin
Zab2
GO positive regulation of TGFβ receptor signaling pathway
negative regulator
positive regulator
control
Blastocystis ST7
J
pSmad3/2
Smad7
fold change
1 control -TGFb
2 control +TGFb
3 I3AA
4 metabolite D8M7V4

Appendix Fig. S2

A. Left: Gel electrophoresis of PCR products amplified from total DNA isolated from *Blastocystis* ST7B and ST7H and large intestine content. Control represents the negative amplification reaction with MQ water instead of DNA template. 16S and 18S primers used in the reactions are indicated on the top of the gel. Middle: Schematic depiction of workflow utilised for isolation of *Blastocystis*-derived metabolites. Right: Detection of the indole compounds (Sigma indole detection kit) in the three different metabolite fractions eluted with 10, 50 and 80% methanol, respectively. **B.** Efficacy of iTreg polarization in the presence of different fractions of *Blastocystis*-derived metabolites. **C**, Representative dot blots depicting phenotype of $CD4^+$ T cells after treatment. **D.** Representative dot blots depicting phenotype of $CD4^+$ T cells after polarization in different concentrations of I3AA and IPA. The concentrations of tryptophan derivatives (µg/ml) used upon culture conditions are indicated on the top of the dot plots. **E**. Division status of the iTreg polarized in the presence of different concentration of ST7B and ST7H metabolites. Total indole or indole derivative concentrations were assessed using Sigma indole detection kit. P-values are indicated with *P<0.05, **P<0.01, ***P<0.001, ****P<0.0001. **F.** Division status of iTreg polarized in the presence of different concentrations of individual indole derivatives (I3AA and IPA). **G.** Division status of iTreg polarized in the presence of different concentrations of FICZ. **H.** Expression of CD103 on the surface of iTreg converted in the presence of different concentrations of I3AA. Experiments were repeated three times. Statistical analysis was performed using a two-tailed t-test with Welch-correction. P-values are indicated. **I.** Changes in expression of positive and negative TGFβ signal regulators in tissues from control and *Blastocystis* ST7 infected groups. **J**. Quantitative analysis of the western blots from Fig 2K.

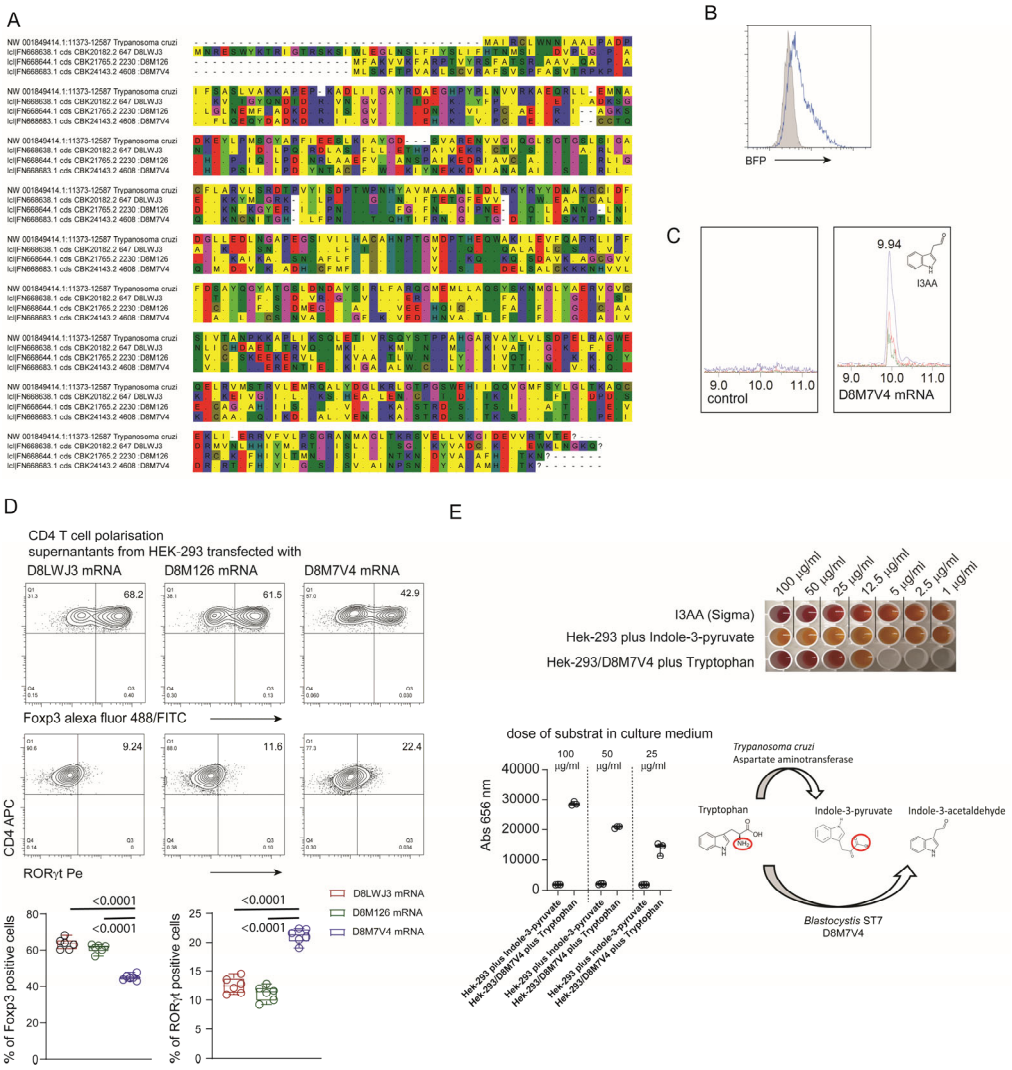

Appendix Fig. S3:

A. Protein sequence alignment. The *Blastocystis* ST7-derived lcl|FN668638.1, lcl|FN668644.1, and lcl|FN668683.1 CDs were compared to *Trypanosoma*-derived TBsASAT (top line). **B.** Positive control for the mRNA transfection. BFP expression in HEK-293 transfected with BFP mRNA. **C.** Characterization of tryptophan metabolites in the medium of HEK-293 cells transfected with D8M7V4 mRNA. **D.** *In vitro* conversion of $CD4^+$ T cells towards iTreg (upper panel) and $ROR\gamma t^+$ Th17 subset (lower panel) in the presence of culture medium derived from HEK-293 transfected with D8LWJ3, D8M126, and D8M7V4, respectively. The experiments comprise 6 replicates. Statistical analysis was performed using a two-tailed t-test with Welch-correction. P-values are indicated. **E.** Analysis of the HEK-293 and D8M7V4-transfected HEK-293 culture supernatant after 72 h culture supplemented with Indole-3-pyruvate (middle row) or tryptophan (lower row), respectively. Upper row, colour reaction of I3AA with Sigma indole detection kit. Different concentrations of I3AA used in detection assay or Indole-3-pyruvate and tryptophan used for culture medium supplementation are indicated on the top. Importantly, Indole-3-pyruvate does not react with indole detection kit. Lower right, hypothetical enzymatic activity of *Blastocystis*-derived D8M7V4 in the context of tryptophan metabolism.

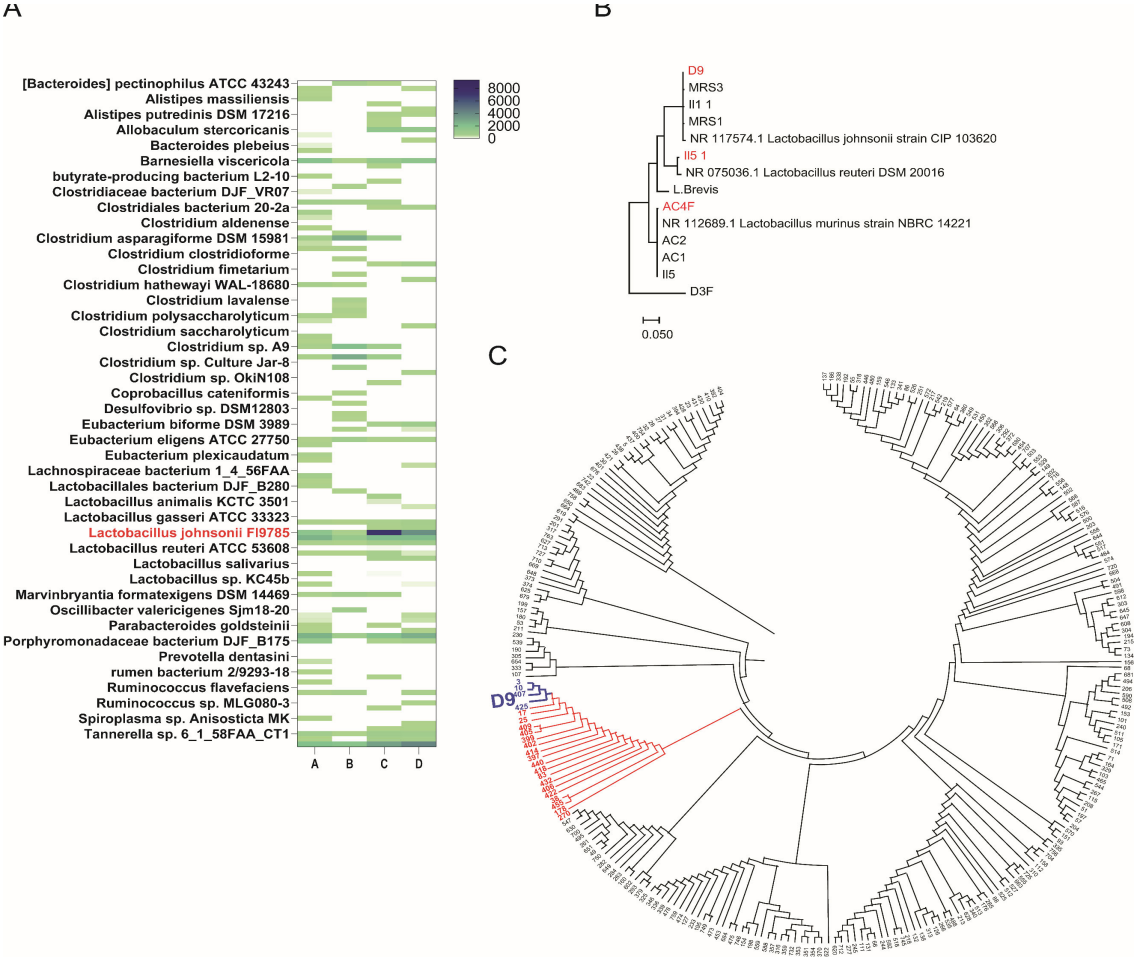

Appendix Fig. S4:

A. Heat map depicting distribution of bacterial species within the gut microbiome from mouse colony utilised for the *in vivo* experiments (four animals). Analysis was done on the reconstructed SSU 16S RNA from data sets after NGS whole 16S sequencing (Materials and Methods). **B.** Neighbor joining tree comparison of the 16S rDNA sequences obtained from bacterial strains isolated from the gut of experimental animals. Each of the whole 16S rDNA sequences were derived from the genomic DNA isolated from individual bacterial isolates. Following PCR amplification with V1-V9 region-specific primers, DNA products were cloned into TOPO vector and sequenced. DNA fragment alignment and estimation of the genetic similarity were done using MUSCLE software with reference 16S rDNA genes (NR 117574.1 for *L. johnsonii,* NR 075036.1 for *L. reuteri* and NR 112689.1 for *L. murinus*). **C.** Alignments of the SSU gene sequences reconstructed from NGS data (**A**) with sequence D9 (highlighted in blue) which were identified as belonging to *L. johnsonii*. In blue, cluster of SSUs with more than 97% similarity to D9 sequence, in red *Lactobacilli* related cluster.

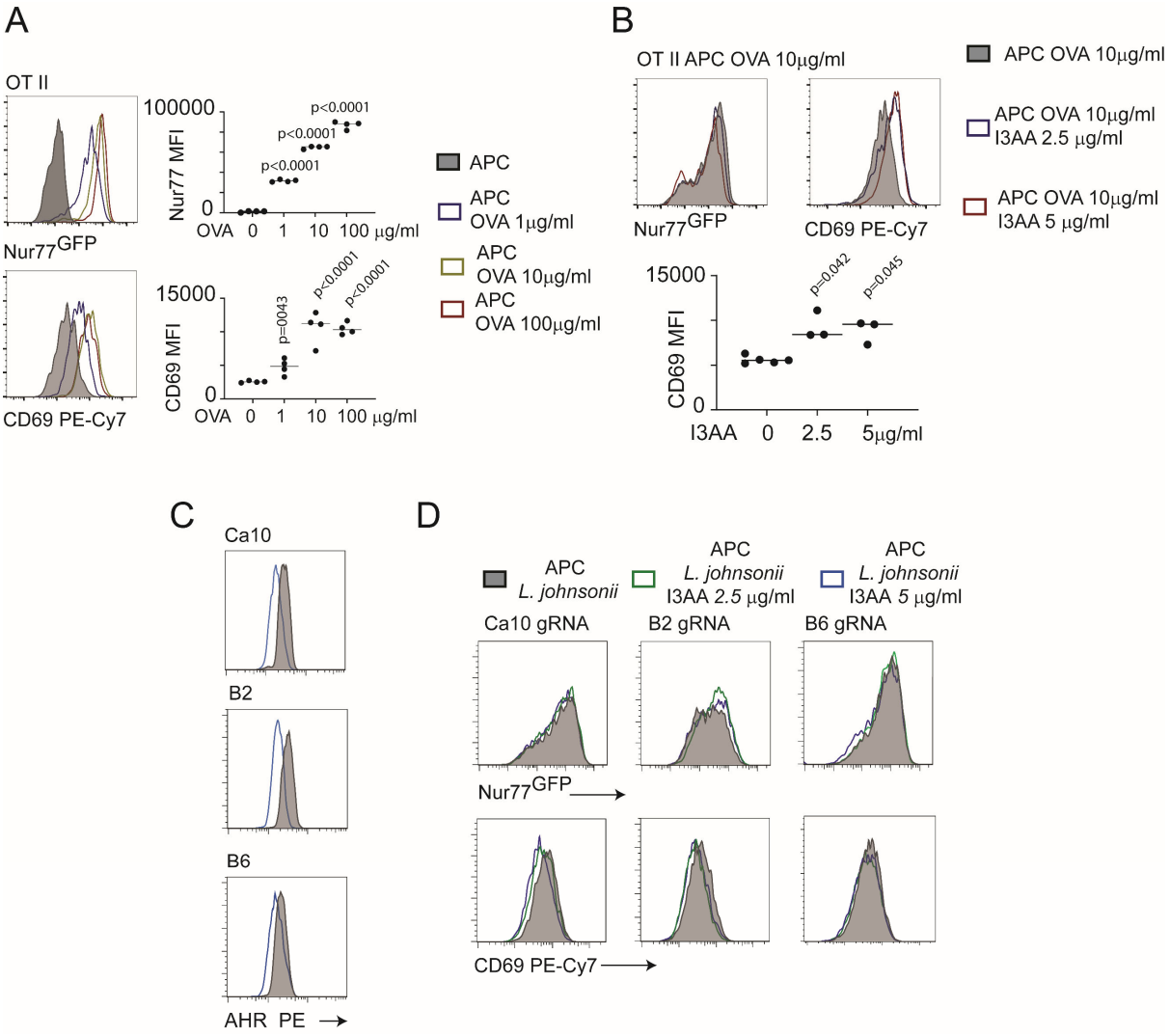

Appendix Fig. S5:

A. Expression of CD69 and Nur77 (measured by Nur77^{GFP} reporter) in OT-II OVA-specific hybridomas upon exposure to bone marrow derived DC pulsed with different concentrations of ovalbumin protein. **B.** Expression of Nur77^{GFP} reporter and CD69 on OT-II hybridomas after exposure to constant concentration of cognate antigen and different concentrations of I3AA. **C.** AhR expression on hybridomas generated after AhR-targeted gene editing. **D.** Representative histograms of Nur77^{GFP} and CD69 expression on AhR-deficient, *L. johnsonii*-specific hybridoma variants after exposure to constant concentrations of cognate antigen and different concentrations of I3AA. Statistical analysis was performed using a two-tailed t-test with Welch-correction. P-values are indicated.

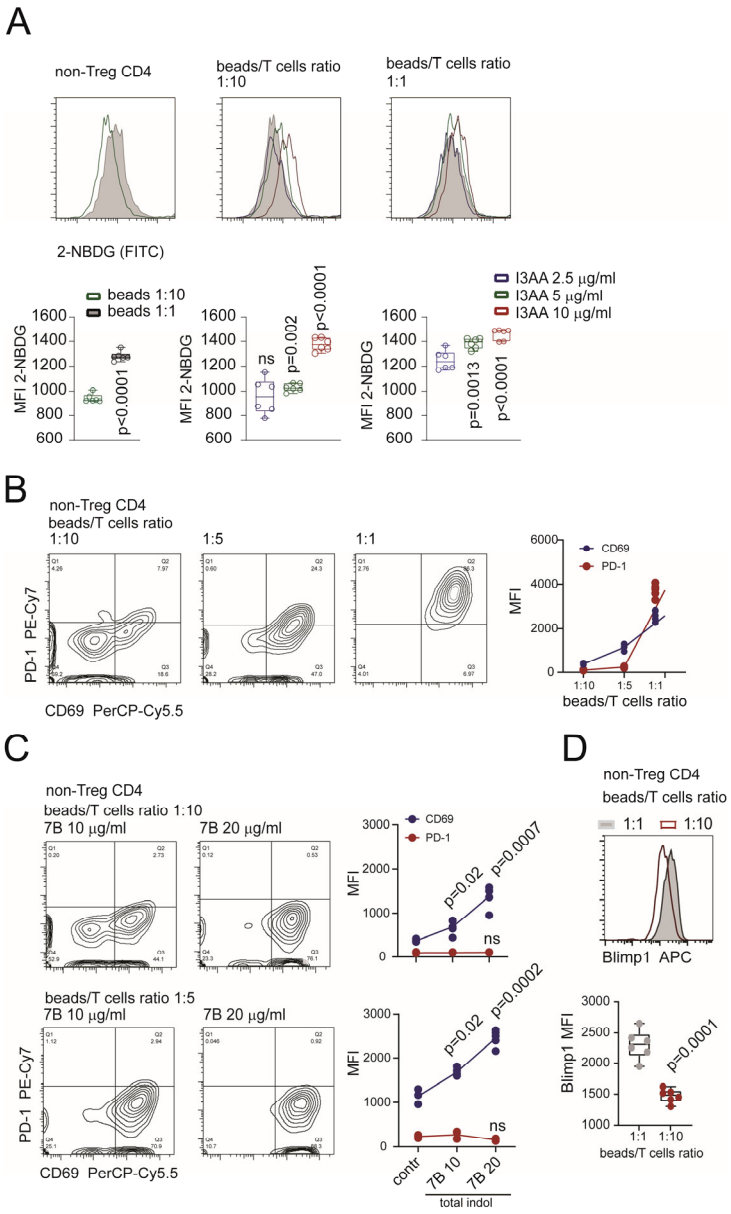

Appendix Fig. S6:

A. Glucose uptake by T cells stimulated with a low (1:10 anti-CD3/CD28 beads/cell ratio) and high (1:1 anti-CD3/CD28 beads/cell ratio) TCR signal. Lower panels: Change in glucose demand by T cells with low and high-saturated TCR signal and increased concentration of I3AA. **B.** Acquisition of CD69 and PD-1 by cells stimulated with different concentrations of TCR stimuli. **C.** Expression of CD69 and PD-1 by T cells experiencing different strengths of TCR stimulation, incubated with indole derivatives isolated from cultures of *Blastocystis* ST7B. **D.** Expression of Blimp-1 in T cells stimulated with low and high dose TCR stimuli. Statistical analysis was performed using a two-tailed t-test with Welch-correction. P-values are indicated. Each group comprised of minimum four replicates from two individual experiments. Right; Blimp-1 expression in T cells stimulated with high dose of TCR stimuli and exposed to *Blastocystis*-derived metabolites.

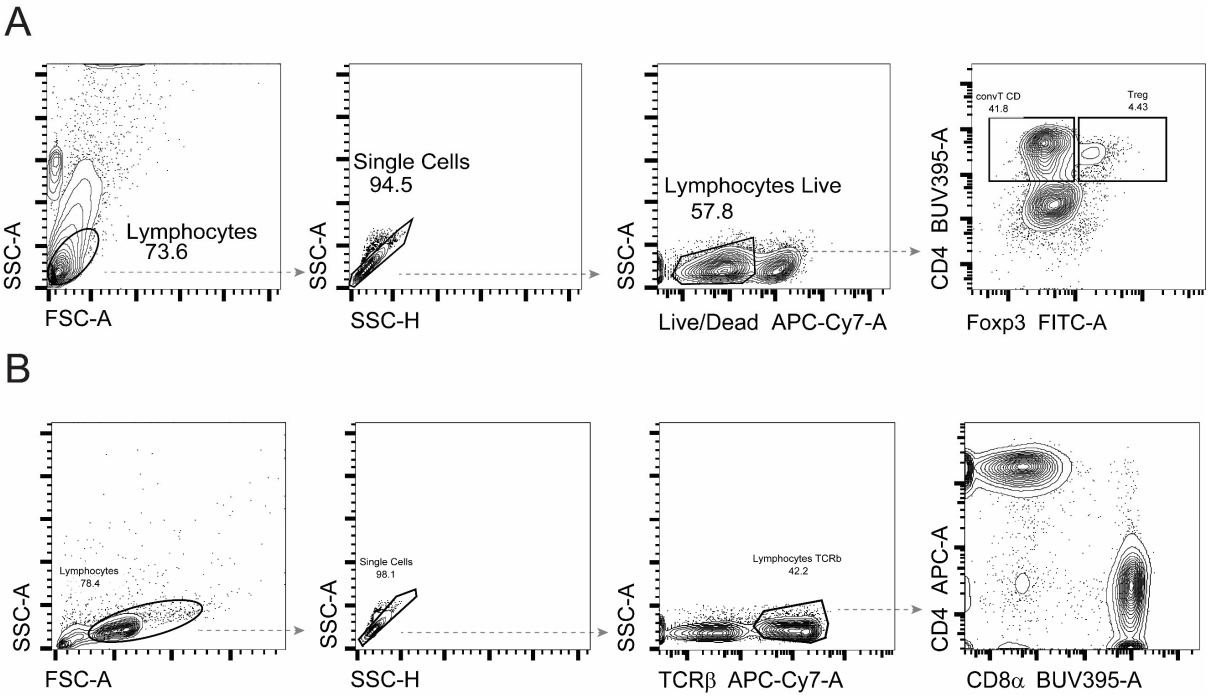

Appendix Fig. S7:

A. Gating strategy of fixed and intracellular stained cells. T cells were isolated from the LP of *Rag2*$^{-/-}$ mice after adoptive transfer of CD4^{+} T cells. The LP cells were stained for live cells prior to fixation and permeabilization using Live/Dead probe. The same gating regime was applied for all experiments in which intracellular staining was performed (LN cells and *in vitro* polarized T cells). **B.** Gating strategy of unfixed (live) cells. The cells were isolated from the LN of *Blastocystis*-infected animals. The same gating regime was applied for all the experiments in which surface staining and analysis of live cells was performed.